

The transparency of the Solar System to the Oort cloud comets

P. A. Dybczyński

Astronomical Observatory of the A. Mickiewicz University, Słoneczna 36, 60-286 Poznań, Poland
e-mail: dybol@amu.edu.pl

Received 4 May 2004 / Accepted 7 August 2004

Abstract. In long-term Monte Carlo simulations of the dynamics of the Oort cloud planetary perturbations cannot be taken directly into account. To do this we propose a simple approximation: estimating the Solar System transparency coefficient P measuring the probability for a comet to be removed from the cloud by planetary perturbations during a single perihelion passage. We estimated the value of this coefficient from the observed and artificial cometary samples. We excluded nongravitational forces from our calculations. We obtained $P \cong 0.25$ for inner cloud comets and $P \cong 0.5$ for the outer and most active part of the cloud. The dependency of P on the comet observability limit OL is also presented for various cometary samples.

Key words. comets: general – Oort cloud – planets and satellites: general

1. Introduction

One method of investigating the source of the observed long period comets is the numerical simulation of the long term dynamical evolution of the bodies in the Oort cloud under the influence of stellar and Galactic perturbations. During such simulations one can observe long term variations in the cometary orbital elements (including the perihelion distance q) due to the permanent action of the Galaxy as well as sudden, sometimes substantial changes due to impulses from passing stars. In this paper we concentrate on another aspect of such simulations, namely the influence of the planetary perturbations during the cometary perihelion passages among Solar System planets.

It is impossible to account for planetary perturbations in an exact manner (e.g. by numerical integration of motion) because the simulation typically extends for 10^6 – 10^9 years and we have no information on the planetary positions during the consecutive perihelion passages of a comet. In some simulations found in the literature (Heisler et al. 1987; Heisler 1990), planetary perturbations were treated in an extremely simplified manner: it was assumed that they always remove a comet from the Oort cloud during the first perihelion passage among planets. Heisler correctly stated that this approach underestimates the number of observable comets because some of them may pass the planetary region without any significant energy change and contribute to the observed flux at the next perihelion. An approximation that accounts for this possibility is needed as planetary perturbations introduce an important and selective mechanism of removing observable comets from the Oort cloud population, as we show below.

In Fig. 1 we present an example of the long term dynamical evolution of the cometary orbit under the influence of the

Galactic disk tide during 40 Myr. It is typical for this kind of evolution that the argument of perihelion ω , the inclination i and perihelion distance q evolve in a strictly synchronous manner: the minima of q and i coincide and ω crosses the 270° or 90° value at the same moment. The vertical lines in Fig. 1 represent changes in the heliocentric distance of a comet. Each vertical line marks one perihelion passage (due to the scale of the horizontal axis the descending and ascending branches overlap – the orbital period for this case is about 1.8 Myr). If we define the observability limit $OL = 2$ AU for the heliocentric distance of a comet during perihelion passage we notice that this comet approaches the Sun closer than the OL 8 times during this single minimum of q . And such a minimum occurs periodically due to the nature of the Galactic tidal perturbation.

When calculating the influx of observable comets we can treat all OL crossings as observable events, or we can count only the first one, assuming that a comet will be removed by planetary perturbations. Neither method reproduces the real situation, as the truth lies somewhere in between: a significant percentage (but not all) is removed and will not be observed at the next perihelion. The simplest way to account approximately for this effect is to use the planetary system transparency coefficient P , defined as the probability for a comet to be removed by planetary perturbations during one perihelion passage. This idea was first introduced in Dybczyński & Prętko (1997). The estimation of the correct value of P is important because if it is too high, our simulated observable long-period comet sample will consist mainly of comets registered during the decreasing phase of q evolution (see Fig. 1), which implies that most of the simulated observable comets will have $0^\circ < \omega < 90^\circ$ or $180^\circ < \omega < 270^\circ$. But the observed long period comets do

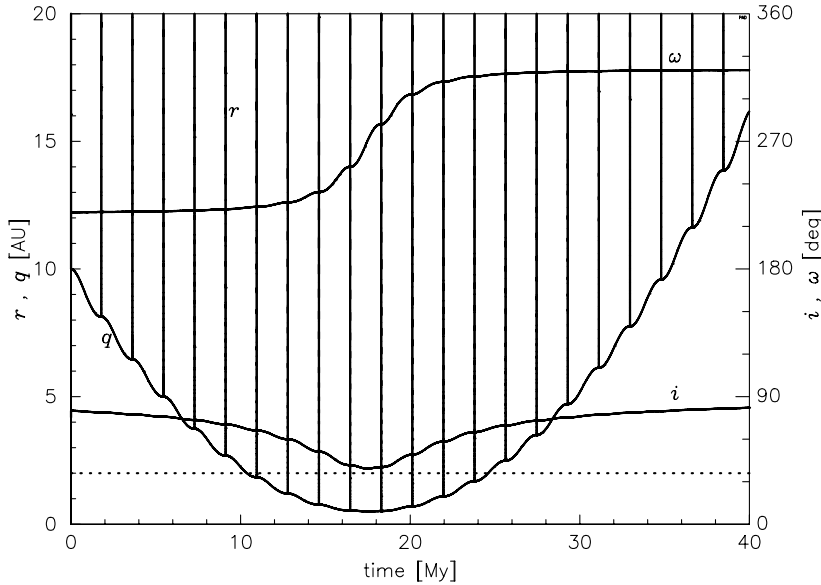


Fig. 1. An example of the orbit evolution under the influence of the Galactic disk tide. In this plot the simultaneous long term evolution of the inclination i and the argument of perihelion ω (both in degrees, see right hand vertical axis) as well as perihelion distance q in AU (left hand vertical axis) are presented. Additionally, changes in the cometary heliocentric distance r are plotted, which produces a series of vertical lines due to the relatively short orbital period with respect to the period of long-term variations. Note that during the single minimum of the perihelion distance this comet crosses the 2 AU dotted line 8 times. Here the semi-major axis $a = 15\,000$ AU.

not have such an asymmetric distribution of ω . If we adopt too small a value of P we will obtain too many passages of comets coming from the inner part of the cloud, which are in reality completely removed by planetary perturbations before they enter the visibility region because owing to their small semi-major-axes the Galactic tide changes their perihelion distances very slowly.

The aim of this paper is to estimate the correct value of the coefficient P basing on the long period comet sample, taken from the 15th edition of the Catalogue of Cometary Orbits (Marsden & Williams 2003, hereafter MW2003) and some numerical experiments. We also present the dependence of P on the cometary semi-major axis and on the assumed observability limit OL .

2. Transparency estimations

The estimation of P based only on original and future inverse semi-major axis values is not sufficient for our purpose. It completely ignores the past and future motion of a comet under the influence of the Galactic disk tide. Starting from the original orbital elements we can integrate numerically the past motion of a comet and calculate its last perihelion distance. Such a calculation and the resulting suggestion to modify the definition of “new” comet was presented by Dybczyński (2001). But similar calculations can be performed for the future motion: starting from the moment at which the comet leaves the planetary system we can follow the motion up to the next perihelion. Some comets will return as observable ($q < OL$) but some will have their perihelion distances increased above the OL by the Galactic disk tide.

Here is where our idea of estimating P comes in. We can perform the numerical integration of the future cometary motion under the influence of the Galactic disk tide twice: first, as proposed above, starting from future elements, second, starting from original orbits and completely ignoring planetary perturbations. By comparing the results of these two different

calculations we can answer the question how the planetary perturbations change the number of comets observable during the next perihelion passage, in other words: what is the probability P that a single long-period comet will be removed by planetary perturbations from the observable sub-population during a single perihelion passage under the simultaneous action of planets and the Galactic disk tide.

2.1. Problem of non-gravitational forces

Before we describe in detail our methods of estimating the transparency coefficient let us discuss the possible influence of non-gravitational forces (NGF) on its value. It is a well known fact that NGF manifest themselves in the motion of some comets. In our calculations NGF might be considered important in two cases. First, when calculating original orbits of observed comets one should account for NGF and use osculating elements determined with the highest accuracy, i.e. with NGF included in the model when possible. Second, when dealing with cloned or simulated comets some approximate formula for NGF might be included in the dynamical model used when calculating a cometary path through the planetary system to obtain future elements.

Taking into account the influence of NGF in the first case mentioned above is practically impossible. The determination of the NGF parameters of a particular comet requires it to be well observed over a very long orbital arc. While there exist many NGF determinations for short period comets (taking advantage of the possibility of linking several apparitions), the number of long period comets for which NGF has been determined is still very small. In the MW2003 catalogue only 23 long period comets have the NGF parameters determined, compared to over 1500 near-parabolic orbits in the general catalogue and to 386 very accurate orbits of classes 1 and 2. Among these 23 orbits 13 are hyperbolic, hence they are excluded from consideration in this paper. In MW2003 they

exclude all near-parabolic comets with NGF determined from the most precise set of orbits and we decided to follow this rule: we limited our calculations to comets from classes 1 and 2 for which the NGF parameters have not been determined according to MW2003.

In the case of cloned and simulated comets only very approximate methods can be used. In general NGF parameters vary significantly from one comet to another and usually evolve with time (even changing their sign). The most popular model of NGF proposed by Marsden et al. (1973) consists of three parameters A_1, A_2, A_3 measuring the non-gravitational force acting on a comet in radial, transversal and binormal direction respectively. The normal component A_3 mainly affects the longitude of the ascending node and the inclination. In almost all cases it is very close to zero if determined at all. A_2 , the transversal component affects mainly the semimajor axis and the eccentricity. However it is typically an order of magnitude smaller than A_1 and can be positive or negative, depending on the direction of the nucleus rotation. Since this direction as well as the orientation of the axis of rotation are distributed isotropically for the long-period comets this component on average can only add some small noise in our calculations with a mean value very close to zero. The largest component A_1 should be positive and describes a radial force which subtracts a very small amount from the gravitational acceleration due to the attraction of the Sun at small heliocentric distances. It mainly affects the argument of perihelion. The Marsden et al. (1973) model is symmetric with respect to the perihelion point, which implies that any semi-major axis perturbation due to this component averages to zero over a full passage through the planetary system and has little or no systematic effect on the orbital distribution of the long-period comets as was clearly demonstrated by Wiegert & Tremaine (1999). They obtained an average perturbation in $1/a$ due to NGF of the order of 10^{-5} AU^{-1} , which is two orders of magnitude smaller than the typical planetary perturbation. After introducing the perihelion asymmetry in this model, see for example Sitarski (1994), one can obtain both positive and negative displacement of the NGF maximum with respect to the perihelion which again on average would reduce to zero. The opinion that NGFs systematically change long-period cometary orbits (see for example Marsden et al. (1978); Yabushita (1991, 1996)) comes partly from the fact that the authors mostly concentrate on the “incoming” half of the cometary orbit, trying to explain negative values of $1/a_{\text{orig}}$. The importance of NGF pointed out by Emel’yanenko & Bailey (1998) comes from the fact, that they use constant NGF parameters and accumulate their effect during thousands of revolutions while we are estimating here the effect of the planetary system during a single perihelion passage. In a recent paper Królikowska (2001) showed that the most important way of taking into account NGF in the motion of the near-parabolic comets is to determine their orbits together with the NGF parameters when possible. She stressed that a long observational arc is required, which makes it possible to obtain reliable values of NGF parameters for only a few percent of the observed long-period comets. She presented new or recalculated non-gravitational orbits for 16 comets, including $1/a_{\text{orig}}$ and $1/a_{\text{fut}}$. These results confirm that on average NGF acts more or less

symmetrically with respect to perihelion, making both original and future orbits “less hyperbolic”.

Remembering that we are constructing a very approximate way of including planetary system perturbations and taking into account all the above arguments we decided not to include NGF in our transparency estimations.

2.2. Estimations from the observed long-period comets

The first comparison was made for 386 comets of classes 1 and 2 (see Marsden et al. 1978) included in MW2003. Using the same high precision dynamical model as in Dybczyński (2001) we calculated both original and future barycentric orbital elements, defined as the osculating barycentric elements at 250 AU from the Sun. In these calculations we used DE406 planetary ephemeris (Standish 1998) with our free ephemeris access software, available at <ftp://ftp.astro.amu.edu.pl/pub/jpleph>. The equations of motion, formulated in a heliocentric, post-Newtonian frame, were integrated numerically using the RA15 routine (Everhart 1985). For testing purposes we compared all calculated $1/a_{\text{orig}}$ and $1/a_{\text{fut}}$ values with those published in MW2003. The results were in excellent agreement, except for the comet C/1962 C1. We calculated $1/a_{\text{orig}} = 0.000033$ for that comet while Marsden & Williams published $1/a_{\text{orig}} = 0.000025$. The reason for this single difference was the accuracy of the published orbital elements. The orbital evolution of this comet is very sensitive to small changes in osculating eccentricity, and modifying it by a small fraction of the last printed digit allows us to reproduce the published $1/a_{\text{orig}}$ value. Probably Marsden & Williams used more decimal places in their calculations than in the printout of the MW2003 catalogue.

We found that 48 comets have never traveled as far as 250 AU from the Sun in their backward motion and as a consequence they were removed from our sample of original orbits. We also excluded 32 comets with hyperbolic original orbits as they formally cannot be treated as comets coming from the Oort cloud. Moreover, for these 32 comets the proposed test cannot be performed as the Galactic disk tide action cannot change an open orbit into a closed one, so all of them will remain unobservable in future in the absence of planetary perturbations. The distribution of $(1/a_{\text{fut}} - 1/a_{\text{orig}})$ for the remaining 306 orbits is shown in Fig. 2 and the general symmetry in planetary perturbations may be easily noted. This sample of comets was divided into four groups of different original semi-major axis range: group I for comets with $a_{\text{orig}} < 1000 \text{ AU}$, group II for $1000 \text{ AU} < a_{\text{orig}} < 10000 \text{ AU}$, group III for $10000 \text{ AU} < a_{\text{orig}} < 50000 \text{ AU}$ and group IV for all remaining elliptical orbits with $a_{\text{orig}} > 50000 \text{ AU}$. Group I consists of dynamically old comets and because of their small semi-major axis (and short orbital period) they are practically immune to Galactic perturbations during one orbit. The only exception is C/1975 V1-A: planetary perturbations changed its semi-major axis from 636 AU to over 34 660 AU and then during one orbital period the perihelion distance increased from 0.19 AU to

Table 1. Distribution of different end-states among 306 long period comets followed forward for one orbital period. The end-states are defined as follows: A – observable (i.e. $q \leq OL$) during current passage, B – observable after one period in the absence of planetary perturbations, C – ejected into hyperbolic orbit by planetary perturbations, D – unobservable after one orbital period (but still elliptic) after including planetary perturbations, E – observable in next perihelion after including planetary perturbations. In the last row of the table the corresponding value of the transparency coefficient $P = (C + D)/B$ is presented.

Group:	$OL = 1$ AU				$OL = 3$ AU				$OL = 5$ AU			
	I	II	III	IV	I	II	III	IV	I	II	III	IV
A	43	21	15	4	98	65	43	13	103	82	73	16
B	43	21	3	0	98	65	22	0	103	82	47	0
C	1	0	0	0	1	0	2	0	1	2	2	0
D	0	4	2	0	0	15	12	0	0	18	26	0
E	42	17	1	0	97	50	8	0	102	62	19	0
P	0.02	0.19	0.67	–	0.01	0.23	0.64	–	0.01	0.24	0.60	–

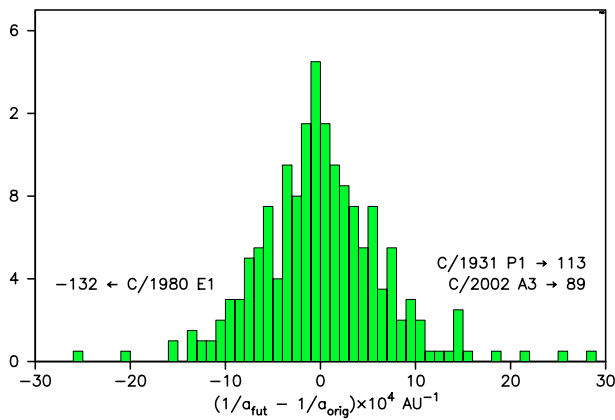


Fig. 2. The distribution of the energy changes (expressed as the inverse of the semi-major axis) due to the planetary perturbations.

15.7 AU due to the Galactic tide. This singular case caused the estimated P to be slightly greater than zero for this group.

On the contrary, group IV contains comets on extremely elongated orbits and as is shown below, all those comets have their perihelion distance increased over the OL by the Galactic disk tide so the estimation of P is impossible in this case. Groups II and III contain typical Oort cloud comets, and may be treated as representing the inner and outer parts of the cloud.

In Table 1 we present the results of our first test, performed for different observability thresholds $OL = 1, 3$ and 5 AU to observe any dependence on this threshold. The sample of orbits is rather small but it is evident that for group II $P \cong 0.2$ and for group III $P \cong 0.6-0.7$. The statistics for $OL = 1$ AU is the worst one so a higher noise is observed.

2.3. Cloning technique

The P value obtained from the statistics of only 306 high precision long period orbits is a rough approximation so we looked for the possibility of improving the statistics. One way is the generation of an artificial cometary sample by increasing the number of comets while reproducing the main characteristics of the observed long-period comet population. We use two consecutive, independent cloning schemes to achieve the population increase.

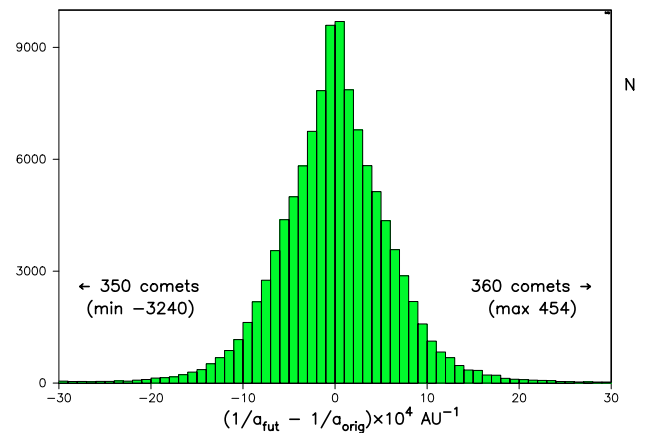


Fig. 3. The distribution of the energy changes (expressed as changes in the inverse of the semi-major axis) due to the planetary perturbations for cloned orbits.

The main agent which produces the observable comets from the Oort cloud is the Galactic disk tide. This perturbation is axi-symmetric with respect to the line perpendicular to the Galactic disk. The orbital evolution under this tidal force is completely independent of the longitude of the ascending node Ω of the cometary orbit in the Galactic frame. So we decided to increase the number of comets by cloning the sample of 306 original cometary orbits used in the first test. We rotate each orbit 36 times around the line perpendicular to the Galactic disk. This was performed by increasing Ω with multiples of 10° with some additional uniform random noise. We generated 36 new sets of orbits obtaining $306 \times 36 = 11\,016$ cloned bodies at this stage.

Next we decided to make our estimations independent of the specific configuration of the planets. We cloned each orbit obtained above 10 further times by adding multiples of the century (again with some random noise) to the osculating epoch of all original barycentric orbits at 250 AU from the sun. This technique spread the observed perihelion passages of comets over almost the whole 6000 year interval covered by the DE406 planetary ephemeris. This superposition of both cloning methods finally generated a set of 110 160 original elements of artificial comets.

Table 2. The same distributions as in Table 1, but obtained for the artificial set of 110 160 comets obtained by the cloning technique described in text.

Group:	$OL = 1 \text{ AU}$				$OL = 3 \text{ AU}$				$OL = 5 \text{ AU}$			
	I	II	III	IV	I	II	III	IV	I	II	III	IV
A	10 440	5760	4680	1440	26 640	19 080	13 320	3600	28 440	24 120	22 680	4680
B	10 440	5760	1513	14	26 640	19 080	7521	68	28 440	24 120	14 608	111
C	38	128	20	0	32	358	124	0	28	449	369	2
D	188	1645	715	9	340	4160	3479	29	368	4876	6668	54
E	10 214	3987	778	5	2668	14 562	3918	39	28 044	18 795	7571	55
P	0.02	0.31	0.49	0.64	0.01	0.24	0.48	0.43	0.01	0.22	0.48	0.50

This cloned set of orbits was tested to see how well it resembles the observed 306 orbit sample. Among others we checked all changes in $1/a$ caused by planetary perturbations, obtaining the distribution presented in Fig. 3, which is almost identical (but smoothed) to that presented in Fig. 2.

2.4. Estimations from cloned comets

Given the set of original orbits described in the previous section we calculated future orbits for all 110 160 cloned comets and then performed two different numerical integrations of future motion under the influence of the Galactic disk tide, starting from original and then from future elements. The results of this extended calculation are presented in Table 2 in the same format as in Table 1. Now the statistics is much better in all groups. For groups I, II the obtained P values are close to that estimated in the previous test. The results for group III show a systematic 10% difference. We will discuss this difference later. Additionally, for cloned sample it was possible to estimate the transparency coefficient for group IV which appeared to be close to that of group III. The comparison of the two P estimations mentioned so far is presented in Fig. 5.

The systematic difference of estimations for group III (observed vs. cloned) needs some explanation: it seems that in this group random comets are more immune to the planetary perturbations than the real ones.

To isolate the problem we separated 91 orbits from group III and performed several future orbit calculations, each time adding some constant time displacement DT to the comet osculating epoch. This way we tested the influence of the planetary system “switched on” at different moments on the same set of 91 cometary orbits with semi-major axes between 10 000 and 50 000 AU. As an approximate measure of the “strength” of planetary perturbations we used the number of ejected comets. Here we treat a comet as being ejected when the eccentricity of its future orbit $e \geq 1$ or when its aphelion $Q \geq 2 \times 10^5$ AU. The results of several such calculations are presented in Table 3.

It is easy to note from Table 3 that the number of ejected comets for $DT = 0$ (which correspond to really observed comets with orbits not modified in any way) is higher than for other displacements. Further analysis revealed that indeed, when tested with these 91 original orbits current planetary system configuration ejects some 10% more comets (50) than in other “phases” (typically 40–45). This effect is clearly present in Fig. 4, where the number of ejected comets is plotted

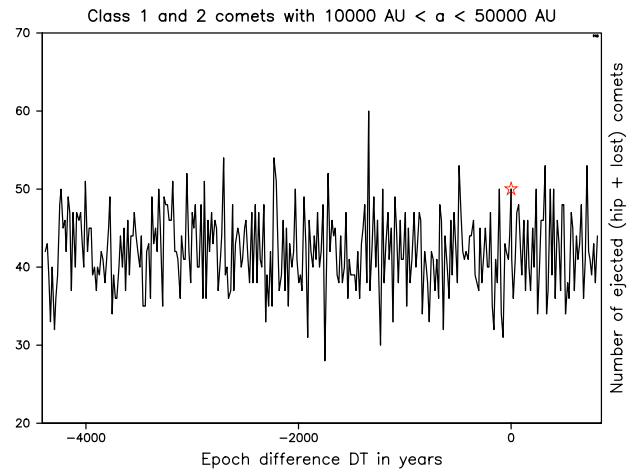


Fig. 4. Number of ejected comets depending on the osculating epoch modification. The star marks the result for the original (not modified) osculating epochs.

Table 3. Different numbers of ejected comets obtained for different “planetary system epochs”. Each row describes the results of 91 future orbit calculations with artificial time displacement DT added to each comet osculating epoch.

$DT[\text{years}]$	$e \geq 1$	$Q \geq 2 \times 10^5$	Total
+500	38	2	40
+200	41	0	41
0	48	2	50
-100	40	2	42
-500	39	1	40
-1000	44	1	45

against DT for all 6000 years spanned by the DE406 JPL planetary ephemeris. It is clearly shown here that the point $DT = 0$ corresponds to the local maximum. This effect is the reason why we obtain a probability of being ejected by planets that is some 10% smaller for cloned orbits than for really observed ones. Additionally, the amplitude presented in Fig. 4 indicates that the accuracy of all P estimations presented in this paper is of order of 10% or so.

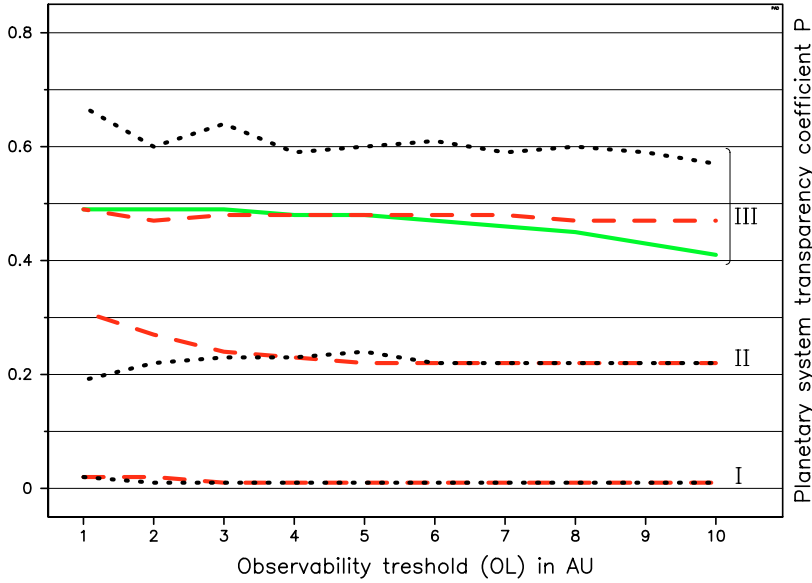


Fig. 5. The transparency coefficients for groups I – III and different observability thresholds (OL) from 1 AU up to 10 AU. The black, dotted line corresponds to the estimations directly from the observed 306 comets while the dark-gray, dashed line describes estimations from the cloned comet sample. In the right part of the plot the corresponding comet groups are marked. The plots presented here are the extended presentation of data included in Tables 1 and 2 respectively. Additionally, for group III the continuous, gray line denotes the results obtained for simulated comets, as described in Sect. 2.5.

Table 4. The same distributions as in Table 1, but obtained for the 187 632 simulated observable comets.

Group:	$OL = 1 \text{ AU}$			$OL = 3 \text{ AU}$			$OL = 5 \text{ AU}$		
	II	III	IV	II	III	IV	II	III	IV
A	20	18 667	261	20	52 155	799	18	86 237	1353
B	20	10 101	1	20	35 358	1	18	63 412	0
C	0	189	0	1	802	0	1	1992	0
D	6	4730	1	8	16 547	1	7	28 412	0
E	14	5182	0	11	18 009	0	10	33 008	0
P	0.30	0.49	1.00	0.45	0.49	1.00	0.44	0.48	–

2.5. Estimations based on simulated comets

As a third approach we estimated the Solar System transparency coefficient using the observable cometary sample, obtained from the numerical simulation of the incoming long-period comet flux. As the numerical model of the Oort cloud we used the classical model based on the results obtained by Duncan et al. (1987). For the detailed description of its construction and main characteristics see Dybczyński (2002), we only mention here that the minimum semi-major axis of simulated comets was 1000 AU. In this simulation we ignored stellar perturbations and follow the dynamical evolution of 4×10^6 randomly chosen comets from the cloud under the influence of the Galactic disk tidal force in a time interval of 500 Myr. We recorded over 2.2 mln perihelion passages below 15 AU for over 90 000 different comets. The obtained sample of cometary orbits was treated as “original” orbits and then the “future” orbits were calculated with the strict planetary system model described in Sect. 2.2. The moment of the perihelion passage was randomly chosen over the time span of the DE 406 planetary ephemeris. Next, as in the previous cases we integrated numerically the motion of each comet under the influence of the Galactic disk tide up to the next perihelion, starting the calculation twice: from “original” and “future” orbital elements. The results of the comparison of these two calculations are presented in Table 4.

Because the source of comets in this case is restricted to the Oort cloud by definition, practically only group III is sufficiently populated, which makes it possible to estimate that $P \cong 0.5$ in this case. The dependency of P for this group obtained for different OL for the simulated comet sample is also presented in Fig. 5 (gray, solid line). We notice here the excellent agreement between the estimations from cloned and simulated samples for group III, especially for small OL values. A slow decrease of P for larger OL is expected because these comets move farther from the main perturber – Jupiter. This cannot be seen either in the observed or the cloned samples because large perihelion distance comets are very rare owing to observational selection; only in the simulated sample are they well represented.

3. Conclusions

We performed several estimations of the planetary system transparency coefficient P defined as the probability that a comet is removed from the observable part of the cloud by planetary perturbations during a single perihelion passage. We discuss non-gravitational perturbations, but decided to ignore them in our calculations. We obtained a good agreement between the different estimations. It seems reasonable to assume that for the inner Oort cloud comets ($a < 10\,000$ AU) this value is close to 25% while for the outer part of the cloud $P \cong 50\%$.

These values should be incorporated in numerical simulations of the source mechanisms for long period comets when the direct calculation of planetary system perturbations is impossible as they can significantly change the orbital element distributions obtained from such a simulation, as was shown by Dybczyński & Prętko (1997) and explained in Fig. 1.

Acknowledgements. I would like to thank Prof. Grzegorz Sitarski, Dr. Tadeusz Jopek, Dr. Sławomira Szutowicz and Dr. Małgorzata Królikowska for helpful discussions during the preparation of this manuscript. I am also indebted to an anonymous referee for valuable suggestions. The research described in this paper was supported by KBN grant No. 2P03D01324 and also partially benefited from KBN grant No. 2P03D00722. This manuscript was prepared with \LaTeX , the open source front-end to the \TeX system.

References

- Duncan, M., Quinn, T., & Tremaine, S. 1987, *AJ*, 94, 1330
 Dybczyński, P. A. 2001, *A&A*, 375, 643
 Dybczyński, P. A. 2002, *A&A*, 396, 283
 Dybczyński, P. A., & Prętko, H. 1997, in *Dynamics and Astrometry of Natural and Artificial Celestial Bodies*, ed. I. M. Wytrzyszczak, J. H. Lieske, & R. A. Feldman (Kluwer Academic Publishers), IAU Coll., 165, 149
 Emel'yanenko, V. V., & Bailey, M. E. 1998, *MNRAS*, 298, 212
 Everhart, E. 1985, in *Dynamics of Comets: Their Origin and Evolution*, ed. A. Carusi, & G. B. Valsecchi (D. Reidel Publishing Company), IAU Coll., 83, 185
 Heisler, J. 1990, *Icarus*, 88, 104
 Heisler, J., Tremaine, S., & Alcock, C. 1987, *Icarus*, 70, 269
 Królikowska, M. 2001, *A&A*, 376, 316
 Marsden, B. G., Sekanina, Z., & Yeomans, D. K. 1973, *AJ*, 78, 211
 Marsden, B. G., Sekanina, Z., & Everhart, E. 1978, *AJ*, 83, 64
 Marsden, B. G., & Williams, G. V. 2003, *Catalogue of Cometary Orbits 15th edition* (Cambridge, Mass.: Smithsonian Astrophysical Observatory)
 Sitarski, G. 1994, *Acta Astron.*, 44, 91
 Standish, E. M. 1998, *JPL Planetary and Lunar Ephemerides, Interoffice Memorandum IOM 312.F – 98 – 048*, Jet Propulsion Laboratory
 Wiegert, P., & Tremaine, S. 1999, *Icarus*, 137, 84
 Yabushita, S. 1991, *Earth Moon and Planets*, 52, 87
 Yabushita, S. 1996, *MNRAS*, 283, 347